

## SPECTROSCOPY OF THE $\Upsilon(2S)$ WITH THE CRYSTAL BALL\*

Joachim Irion

(representing the Crystal Ball Collaboration)<sup>1</sup>

*Physics Department, Harvard University*

*Cambridge, Massachusetts 02138*

*and*

*Stanford Linear Accelerator Center*

*Stanford University, Stanford, California 94305*

### ABSTRACT

The Crystal Ball experiment has been taking data at the DORIS II storage ring at DESY/Hamburg on the  $\Upsilon(2S)$  and  $\Upsilon(1S)$  resonances since Summer 1982. Results on the hadronic transitions between the  $\Upsilon(2S)$  and the  $\Upsilon(1S)$  are presented as well as measurements of the radiative decays of the  $\Upsilon(2S)$  to the  $\chi_b$  states in inclusive and exclusive channels. The exclusive  $\Upsilon(2S) \rightarrow \gamma\chi_b \rightarrow \gamma\gamma\Upsilon(1S) \rightarrow \gamma\gamma l^+l^-$  sample allows a study of the spins of the  $\chi_b$  states. Also discussed is the present status of the  $\zeta(8.3)$  in the radiative decays of the  $\Upsilon(1S)$ .

### 1. INTRODUCTION

The family of  $\Upsilon$  resonances are bound states of the  $b\bar{b}$  system. Many properties of these states can be calculated with the help of QCD inspired potential models and thus measurements of these properties provide interesting tests of QCD predictions<sup>2</sup>. We report here a study of several of the major transitions from the  $\Upsilon(2S)$  (the  $2\ ^3S_1$  state in spectroscopic notation) shown in Fig. 1. The center-of-gravity of the triplet P states (also called  $\chi_b$  states) is determined by the small range behavior of a given model and the splitting of the states is due to spin-orbit and tensor terms. The  $1\ ^1S_0$  and  $2\ ^1S_0$  states ( $\eta_b, \eta'_b$ ) have not yet been observed; the energy difference between corresponding  $1\ ^1S_0$  and  $3\ ^3S_1$  states is determined by the spin-spin interaction.

Another test of QCD is performed by studying the hadronic  $\pi\pi$  decays of the  $\Upsilon(2S)$  down to the  $\Upsilon(1S)$ . Branching ratios and invariant mass distributions of the  $\pi\pi$  system are compared to theoretical predictions.

---

\* Work supported in part by the Department of Energy under contracts DE-AC02-76ER03064 (Harvard) and DE-AC03-76SF00515 (SLAC).

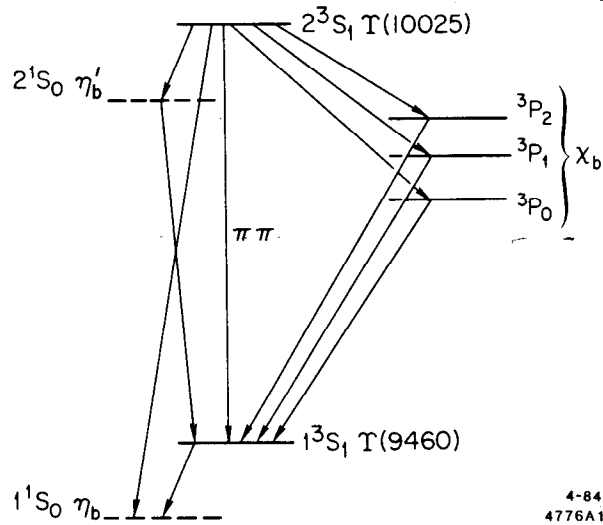


Fig. 1. The level scheme for  $b\bar{b}$  bound states below the  $\Upsilon(2S)$ .

The Crystal Ball detector at the DORIS II storage ring at DESY is particularly suited to study these phenomena. It is a well understood, nonmagnetic detector; detailed descriptions can be found in References 3 and 4. It is essentially a highly segmented shell of NaI crystals covering more than 94% of  $4\pi$ . Directions of charged particles are measured with proportional tube chambers.

The energy of photons and electrons is measured with a resolution of  $\frac{\sigma(E)}{E} = \frac{(2.7 \pm 0.2)\%}{E^{1/4}(GeV)}$  and their emission angle is determined with a resolution of  $1-2^0$ . Non interacting charged particles deposit usually  $\simeq 210$  MeV into 1-2 crystals but the energy distribution also has a tail towards higher energies due to nuclear interactions.

During 1982-1984 the Crystal Ball accumulated  $\simeq 200 \cdot 10^3$   $\Upsilon(2S)$  decays corresponding to an integrated luminosity of  $\int L dt \simeq 61 pb^{-1}$ . The  $\Upsilon(2S)$  run was interspersed with data taking on the  $\Upsilon(1S)$  yielding  $\simeq 300 \cdot 10^3$  resonance decays ( $\int L dt \simeq 33 pb^{-1}$ ) and some data taking on the continuum below the  $\Upsilon(1S)$  resonance ( $\int L dt \simeq 4.5 pb^{-1}$ ).

In the following sections measurements of hadronic  $\Upsilon(2S)$  decays and inclusive and exclusive radiative photon transitions from the  $\Upsilon(2S)$  will be described. We will also discuss the status of the  $\zeta(8.3)$ . The analysis techniques to study the various phenomena can only be sketched. For more detailed information the reader will be referred to the individual references.

## 2. HADRONIC TRANSITIONS

The  $\pi\pi$  transitions from the  $\Upsilon(2S)$  can be viewed as a two stage process in which 2 gluons are radiated from this excited state and subsequently fragment into two pions (see Fig. 2). The Crystal Ball can measure this process through the reactions  $\Upsilon(2S) \rightarrow \pi^0\pi^0\Upsilon(1S)$  and  $\Upsilon(2S) \rightarrow \pi^+\pi^-\Upsilon(1S)$ ,  $\Upsilon(1S) \rightarrow l^+l^-$ .

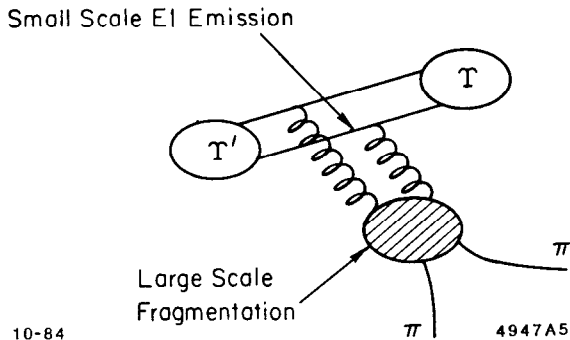


Fig. 2. Elements of the Process  $\Upsilon(2S) \rightarrow \pi\pi\Upsilon(1S)$ .

### The Reaction $\Upsilon(2S) \rightarrow \pi^0\pi^0\Upsilon(1S) \rightarrow \pi^0\pi^0(e^+e^- \text{ or } \mu^+\mu^-)$ (Ref. 5)

The analysis requires that there are exactly 6 particles well within the solid angle of the Ball, two of which (the lepton candidates) are nearly back to back with a signature typical of muons (minimum ionizing) or high energy electrons. The remaining 4 particles are considered to be candidates for photons from the  $\pi^0\pi^0$  decay and have to exhibit a lateral energy distribution in the crystals compatible with showers of electromagnetically interacting particles. To ensure good energy measurements of the photons all particles have to be well separated from each other.

Events surviving these cuts are then fit to the hypothesis  $\Upsilon(2S) \rightarrow \gamma\gamma\gamma\gamma l^+l^-$  using energy- and momentum conservation (a 2-C fit).<sup>#1</sup> For events passing the fit we plot the 2 photon invariant mass  $m_{\gamma\gamma}$  for each pairing combination versus the invariant mass of the other photon pair (Fig. 3). There are 3 entries per event. A clear clustering of events in the region of  $2\pi^0$ 's is observed. To reduce background a cut of  $\pm 22$  MeV (corresponding to  $3\sigma$ ) on both  $m_{\gamma\gamma}$  is applied, as indicated. For events inside the box we calculate the mass difference  $\Delta M = M_{\Upsilon(2S)} - M_{l^+l^-}$ , where  $M_{l^+l^-}$  is the mass recoiling against the 4  $\gamma$  system, calculated from the measured photon momentum vectors. The distribution of  $\Delta M$  (shown in Fig. 4) has a clean peak centered at the  $\Upsilon(2S) - \Upsilon(1S)$  mass difference.

<sup>#1</sup> We only use the directions of the leptons.

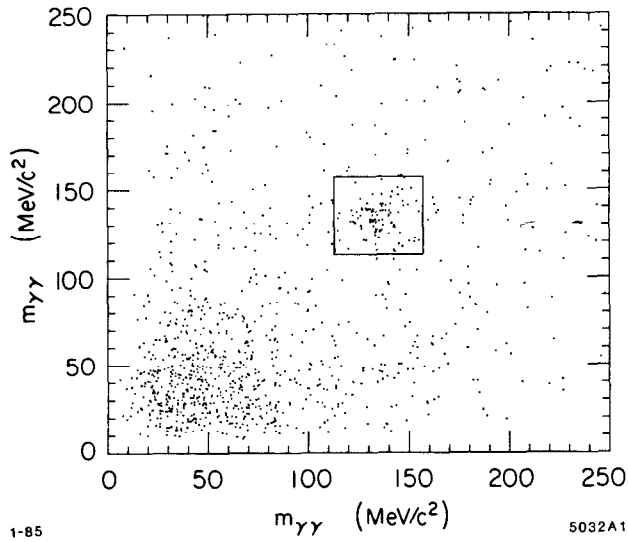


Fig. 3. Scatter plot of the observed  $m_{\gamma\gamma}$  masses of the  $\gamma\gamma\gamma\gamma\mu^+\mu^-$  and  $\gamma\gamma\gamma\gamma e^+e^-$  samples. There are 3 entries per event. The box indicates the boundaries for the cut.

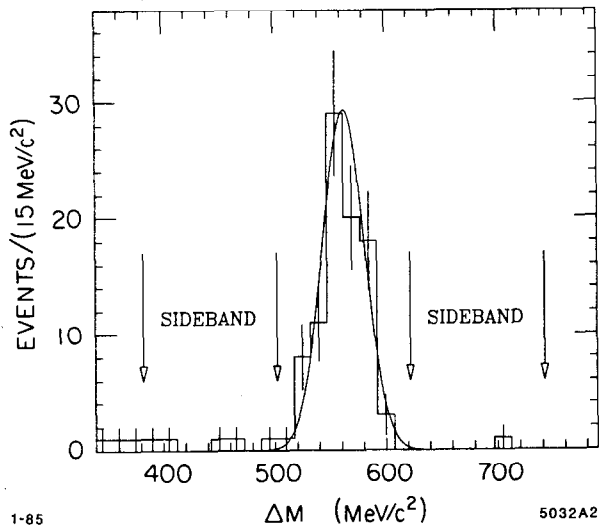


Fig. 4. The mass difference  $\Delta M = M_{\Upsilon(2S)} - M_{l+l-}$ , where  $M_{l+l-}$  is the mass recoiling against the 4  $\gamma$  system. The solid curve is the Monte Carlo expectation from energy- and angular resolution.

The final sample contains 44 events of the  $\gamma\gamma\gamma\gamma\mu^+\mu^-$  type and 46 events of the type  $\gamma\gamma\gamma\gamma e^+e^-$  between  $503 \leq \Delta M \leq 623$  MeV. The background, estimated from side bands and in agreement with Monte Carlo studies, is 2 events in the  $e^+e^-$  channel and 1 event in the  $\mu^+\mu^-$  channel. The overall detection

efficiency is calculated by Monte Carlo studies to be  $\epsilon_{\pi^0\pi^0ee} = (10 \pm 1)\%$  and  $\epsilon_{\pi^0\pi^0\mu\mu} = (9 \pm 1)\%$ . The branching ratios are given in Table I.

It is interesting to study the invariant  $\pi^0\pi^0$  mass distribution as there are theoretical predictions based on QCD for its shape. Our data is shown in Fig. 5. Phasespace (dashed line) is clearly excluded; Fits to the mass distribution with three different theoretical models<sup>6,7,8</sup> give essentially the same prediction (solid line) and provide a good description of the data.

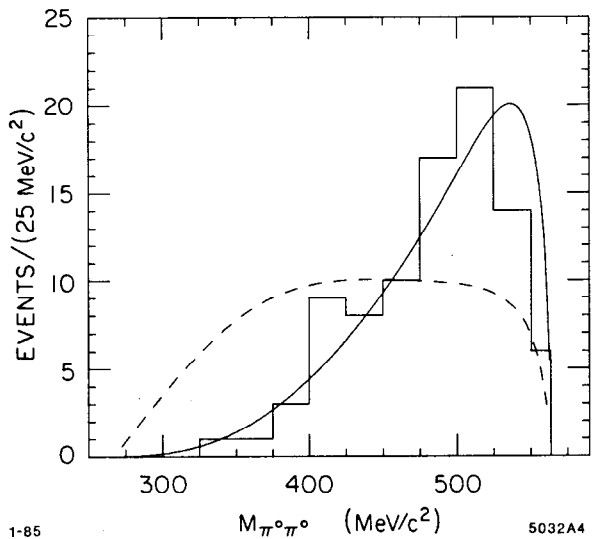


Fig. 5. The invariant  $\pi^0\pi^0$  mass distribution. The solid curve represents fits of the theoretical expressions to the data.

#### The Reaction $\Upsilon(2S) \rightarrow \pi^+\pi^-\Upsilon(1S) \rightarrow \pi^+\pi^-e^+e^-$ (Ref. 5)

The analysis of the reaction  $\Upsilon(2S) \rightarrow \pi^+\pi^-\Upsilon(1S) \rightarrow \pi^+\pi^-e^+e^-$  is quite similar to the one described above. The requirements for the  $e^+e^-$  pair are essentially the same. The main difference is a  $\pi^+\pi^-$  signature instead of the four photons. These events are then subjected to a 3-C kinematic fit to test the  $\Upsilon(2S) \rightarrow \pi^+\pi^-e^+e^-$  hypothesis.<sup>#2</sup> A final sample of 169 events survives all cuts. Monte Carlo studies indicate a total of 8 background events.

The overall detection efficiency is estimated to be  $\epsilon_{\pi^+\pi^-e^+e^-} = (17 \pm 3)\%$ . The branching ratios are listed in Table I. Recalling the corresponding result for the  $\pi^0\pi^0$  channel we calculate the ratio  $\frac{\Gamma(\Upsilon(2S) \rightarrow \pi^0\pi^0\Upsilon(1S))}{\Gamma(\Upsilon(2S) \rightarrow \pi^+\pi^-\Upsilon(1S))} = 0.47 \pm 0.11$ , consistent with isospin conservation.

<sup>#2</sup> The constraints are energy and momentum conservation and the  $e^+e^-$  pair is constrained to the  $\Upsilon(1S)$  mass.

**Table I**Branching ratios for hadronic decays  $\Upsilon(2S) \rightarrow \pi\pi\Upsilon(1S)$   $\Upsilon(1S) \rightarrow l^+l^-$ .

$\pi^0\pi^0$ - channel:
$B(\Upsilon(2S) \rightarrow \pi^0\pi^0\Upsilon(1S)) \cdot B(\Upsilon(1S) \rightarrow e^+e^-) = (2.2 \pm 0.4 \pm 0.2) \cdot 10^{-3}$
$B(\Upsilon(2S) \rightarrow \pi^0\pi^0\Upsilon(1S)) \cdot B(\Upsilon(1S) \rightarrow \mu^+\mu^-) = (2.4 \pm 0.4 \pm 0.3) \cdot 10^{-3}$
Average:
$B(\Upsilon(2S) \rightarrow \pi^0\pi^0\Upsilon(1S)) \cdot B(\Upsilon(1S) \rightarrow l^+l^-) = (2.3 \pm 0.3 \pm 0.3) \cdot 10^{-3}$
$B(\Upsilon(2S) \rightarrow \pi^0\pi^0\Upsilon(1S)) = (8.0 \pm 1.5)\%$ <sup>a)</sup>
$\pi^+\pi^-$ - channel:
$B(\Upsilon(2S) \rightarrow \pi^+\pi^-\Upsilon(1S)) \cdot B(\Upsilon(1S) \rightarrow e^+e^-) = (4.9 \pm 0.4 \pm 1.0) \cdot 10^{-3}$
$B(\Upsilon(2S) \rightarrow \pi^+\pi^-\Upsilon(1S)) = (16.9 \pm 4.0)\%$ <sup>a)</sup>

a) Using  $B_{ll}(\Upsilon(1S)) = (2.9 \pm 0.3)\%$ , see Ref. 5.

### 3. PHOTON TRANSITIONS

The Crystal Ball can study the  $\gamma$  transitions from the  $\Upsilon(2S)$  in two different ways: *i*) Through the inclusive reaction  $\Upsilon(2S) \rightarrow \gamma + \text{hadrons}$ , observing monochromatic photon lines in the inclusive photon spectrum, or *ii*) through the exclusive channel  $\Upsilon(2S) \rightarrow \gamma\chi_b \rightarrow \gamma\gamma\Upsilon(1S) \rightarrow \gamma\gamma$  ( $e^+e^-$  or  $\mu^+\mu^-$ ). Both methods are complementary approaches: *i*) yields the branching ratios for  $\Upsilon(2S) \rightarrow \gamma\chi_b$  transitions whereas *ii*) measures the product branching ratios for the  $\Upsilon(2S) \rightarrow \gamma\chi_b \rightarrow \gamma\gamma\Upsilon(1S)$  cascade and therefore with *i*) also yields the branching ratio  $B(\chi_b \rightarrow \gamma\Upsilon(1S))$ .

#### Inclusive Photon Analysis (Ref. 9)

The task is to find single, monoenergetic  $\gamma$ 's in a complicated multi-hadron environment. To achieve this goal a number of cuts are introduced to suppress various sources of backgrounds such as charged particles, photons from  $\pi^0$  decays and photons whose electromagnetic energy showers are contaminated by energy deposits from near-by particles. A photon candidate must be neutral as determined by the chambers, its lateral energy distribution in the crystals must agree with what is expected from an electromagnetic shower and it must be well separated from other particles. Also it may not form a  $\pi^0$  with an other photon. The overall selection efficiency is  $\simeq 13\%$  estimated by Monte Carlo studies.

In Fig. 6 the inclusive photon spectrum from the  $\Upsilon(2S)$  is shown. Three clearly separated peaks in the region between 100-170 MeV and another around 430 MeV are visible. The shoulder at 210 MeV is due to misidentified charged particles. We interpret the peaks below 170 MeV as the primary transitions from the  $\Upsilon(2S)$  to the  $^3P_{2,1,0}$  states and the structure at 430 MeV as the secondary transitions from the  $^3P_{2,1}$  states to the  $\Upsilon(1S)$ .

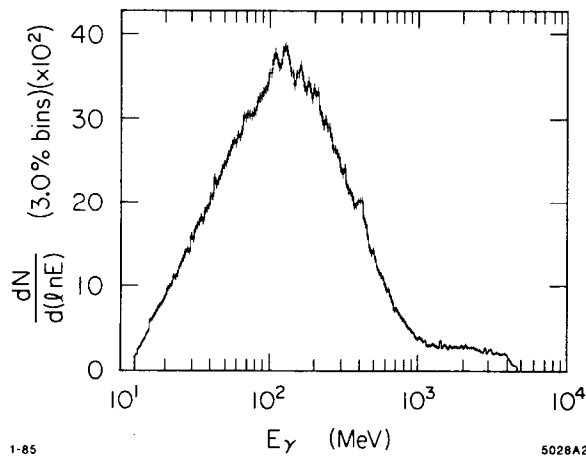


Fig. 6. The inclusive photon spectrum from hadronic  $\Upsilon(2S)$  decays.

To extract the signals we fit the spectrum between  $\simeq 50$  and  $\simeq 650$  MeV with the sum of the following terms: A fourth order Legendre polynomial (to represent the photon background), a charged particle spectrum (to accommodate the punch-through), three Gaussians with their widths given by our resolution (to describe the signals between 100-170 MeV) and two more Gaussians (to describe the Doppler broadened secondary transitions), with their positions fixed by the energies of the primary lines and the known  $\Upsilon(2S) - \Upsilon(1S)$  mass difference.

The fit, shown in Fig. 7, has a confidence level of 72%. The fitted energies, number of photons in the peaks and the resulting branching ratios are listed in Table II.

#### Exclusive Photon Analysis (Ref. 10)

The event selection for the reaction  $\Upsilon(2S) \rightarrow \gamma\gamma\Upsilon(1S) \rightarrow \gamma\gamma(e^+e^- \text{ or } \mu^+\mu^-)$  is similar to the hadronic  $\Upsilon(2S) \rightarrow \pi^0\pi^0l^+l^-$  analysis. Four particles are required in the Ball. Two of them have to have the signature of the back-to back lepton pair (as in the  $\pi^0\pi^0ll$  case). The remaining two particles must be neutral and have their energy deposited in the crystals as expected from photons. All four particles must be well separated from each other.

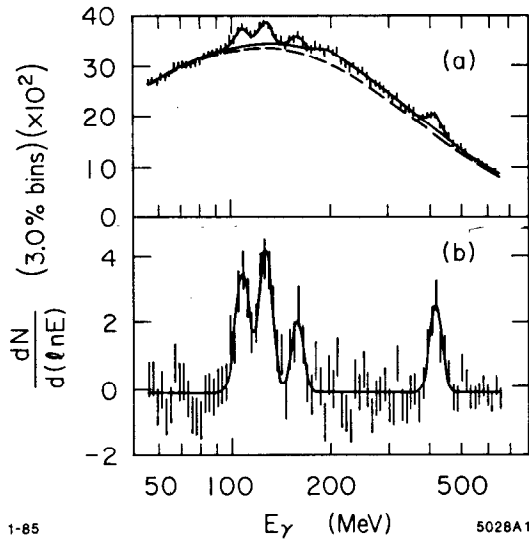


Fig. 7. (a) The fitted part of the photon spectrum. The curves represent the results of the fit. (b) The same distribution after background subtraction.

Events with this topology are subjected to a 2-C kinematic fit to the hypothesis  $\Upsilon(2S) \rightarrow \gamma\gamma l^+l^-$ , using energy and momentum conservation.<sup>#3</sup> A total of 282 events pass.

A plot of  $E_{\gamma \text{ low}}$  (defined as the lowest of the two photon energies) vs. the mass difference  $\Delta M = M_{\Upsilon(2S)} - M_{l^+l^-}$ , where  $M_{l^+l^-}$  is the mass recoiling against the two photons, is shown in Fig. 8. Two distinct clusters in  $E_{\gamma \text{ low}}$  are observed in the region of  $\Delta M \simeq 560$  MeV, which indicates that indeed we do measure the photon transitions from the  $\Upsilon(2S)$  to the  $\Upsilon(1S)$ . Eliminating all events outside the interval  $562 \pm 48$  MeV leaves a sample of 58  $\gamma\gamma ee$  events and 42  $\gamma\gamma\mu\mu$  events. The efficiency is calculated by Monte Carlo and is of the order of  $\simeq 20\%$  (depending on spin). In Fig. 9 we plot  $E_{\gamma \text{ low}}$  for the final sample. Also shown is a fit to the two well separated lines, which are interpreted to be the transitions to the  ${}^3P_2$  and  ${}^3P_1$  states. Note that in contrast to the result from the inclusive reaction there is no indication of a third photon line. This is expected as the  ${}^3P_0 \rightarrow \gamma\Upsilon(1S)$  transition is supposed to be suppressed. The fitted number of signal events and the corresponding branching ratios are presented in Table II.

Comparing the photon energies measured in the exclusive channel to the ones from the inclusive analysis we find that the results agree within their errors.

<sup>#3</sup> We only use the directions of the leptons.

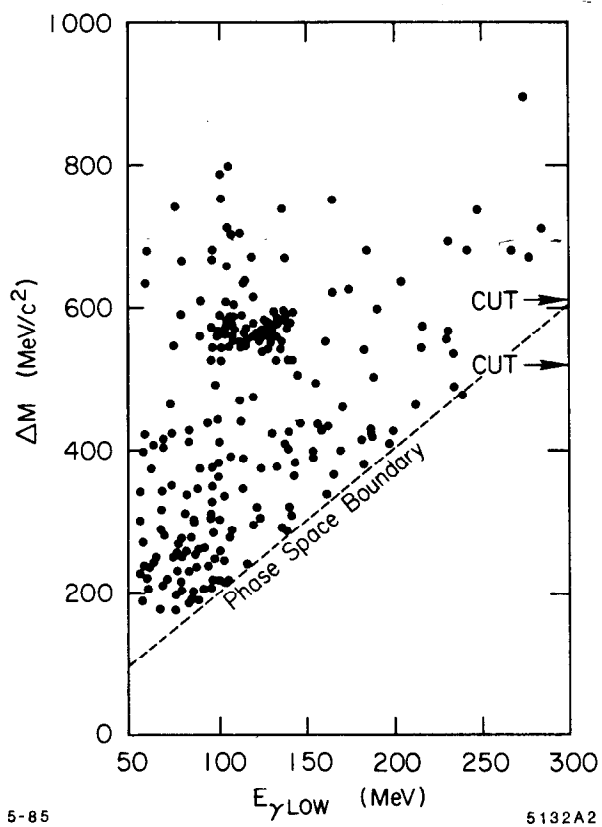


Fig. 8. Scatter plot of the lowest of the two photon energies versus the mass difference  $\Delta M = M_{T(2S)} - M_{ll}$ . The arrows indicate the cut on  $\Delta M$ .

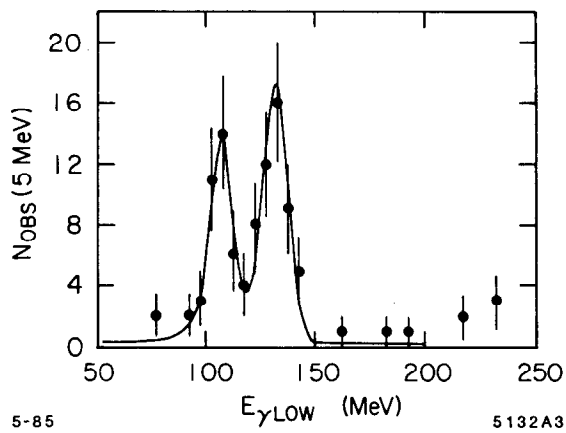


Fig. 9. Projection of the signal band in Fig. 8 on the  $E_{\gamma \text{ low}}$  axis. The curve represents a fit to the data.

Hence we can average the two independent results and obtain the values given in Table II. Our results are compared with other experiments<sup>11,12,13</sup> in Fig.10. All four experiments report values for the  $^3P_{2,1}$  states that are in agreement with each other. For the mass of the  $^3P_0$  state, however, our results disagree with CUSB<sup>11,12</sup> and preliminary ARGUS results<sup>13</sup> by about 2 standard deviations<sup>14</sup>. Also indicated are some theoretical predictions<sup>15,16,17,18</sup>. A quantity of interest to theorists is the ratio  $r = \frac{M_2 - M_1}{M_1 - M_0}$ .<sup>14</sup> We obtain  $r = 0.61 \pm 0.10$ .

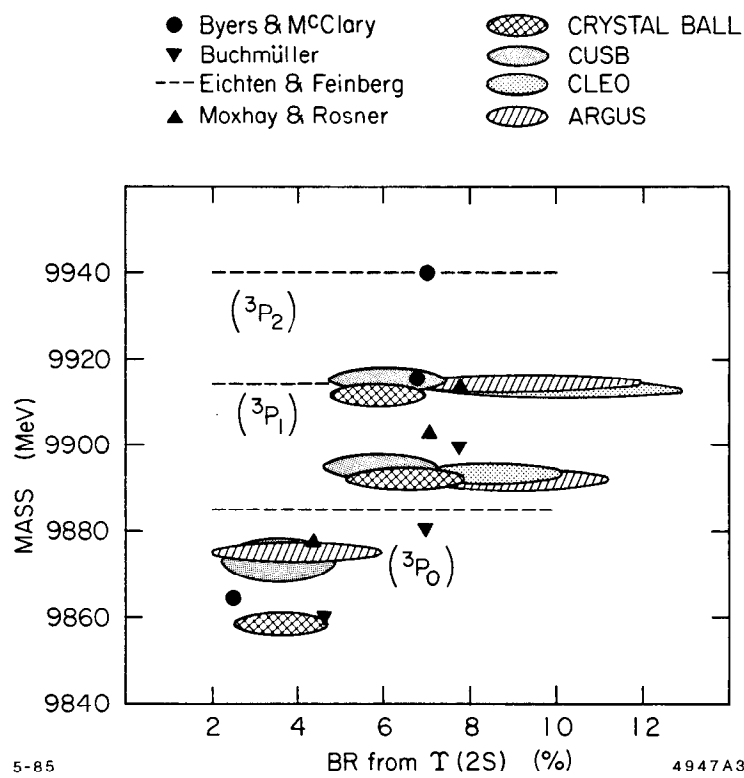


Fig. 10. Experimental and theoretical values for branching ratios of  $\Upsilon(2S) \rightarrow ^3P_{2,1,0}$  transitions and masses of the  $P$  states as calculated from the photon energies.

<sup>14</sup> We use the inclusive results to calculate  $r$ .

**Table II**  
Radiative Transitions of  $\Upsilon(2S)$ .

Transition	Photon Energy (MeV)	Number of Photons	Efficiency <sup>a)</sup> (%)	Branching Ratio
Inclusive Analysis: $\Upsilon(2S) \rightarrow \gamma + X$				
$^3P_2$	$110.4 \pm 0.8 \pm 2.2$	$1444 \pm 176$	13	$(5.8 \pm 0.7 \pm 1.0)10^{-2}$
$^3P_1$	$130.6 \pm 0.8 \pm 2.4$	$1710 \pm 178$	14	$(6.5 \pm 0.7 \pm 1.2)10^{-2}$
$^3P_0$	$163.8 \pm 1.6 \pm 2.7$	$799 \pm 170$	12	$(3.6 \pm 0.8 \pm 0.9)10^{-2}$
	$< 430 >$	$851 \pm 168$	13	$(3.6 \pm 0.7 \pm 0.5)10^{-2}$
Exclusive Analysis: $\Upsilon(2S) \rightarrow \gamma\chi_b \rightarrow \gamma\gamma l^+l^-$				
$^3P_2$	$107.0 \pm 1.1 \pm 1.3$	$35 \pm 7$	20	$(4.4 \pm 0.9 \pm 0.6)10^{-4}$
$^3P_1$	$131.7 \pm 0.9 \pm 1.0$	$53 \pm 8$	23	$(5.8 \pm 0.9 \pm 0.7)10^{-4}$
$^3P_0$	150 – 200	$< 2.8$	19	$< 0.4 \cdot 10^{-4}$ (90% C.L.)
Combining Inclusive and Exclusive Results				
	Photon Energy (MeV) <sup>b)</sup>		Branching Ratio (%) <sup>c)</sup>	
$^3P_2$	$108.2 \pm 1.6$		$B(^3P_2 \rightarrow \gamma\Upsilon(1S)) = (28 \pm 6 \pm 5)\%$	
$^3P_1$	$131.5 \pm 1.4$		$B(^3P_1 \rightarrow \gamma\Upsilon(1S)) = (32 \pm 6 \pm 6)\%$	
$^3P_0$	$163.8 \pm 3.1$		$B(^3P_0 \rightarrow \gamma\Upsilon(1S)) < 4\%$ (90% C.L.)	

a) The efficiency includes effects from the expected angular distribution of the photons. The systematic error is  $\simeq 20\%$  in the inclusive analysis and  $\simeq 13\%$  in the exclusive analysis.

b) Weighted averages. Statistical and systematic errors added in quadrature. For the energy of the  $^3P_0$  transition only the inclusive value is available.

c) Using  $B_{ll}(\Upsilon(1S)) = (2.8 \pm 0.3)\%$  and the branching ratios for the primary transitions measured in the inclusive analysis.

#### Spin Determination of the $\chi_b$ States (Ref. 19)

— In the previous paragraphs we implicitly assumed that the observed photon lines correspond to transitions to the  $\chi_b$  states as shown in Fig. 1. While these assumptions certainly are plausible it is important to measure the spin of the states experimentally.

The uniform acceptance over a large solid angle of the Crystal Ball and its good energy and angular resolution allow the study of correlations of the two observed  $\Upsilon(2S) \rightarrow \gamma\gamma l^+l^-$  cascades, which are almost completely separated in energy. The spins of the  $\chi_b$  states are determined from the complete angular correlations of the final state particles (including the transverse beam polarization).

The analysis will be described with the help of Fig. 11, which serves as an example of a likelihood test for spin 0 of the line at  $\simeq 131$  MeV (expected spin  $J=1$ ). The Gaussian curves represent predictions of the distributions of the test function  $\frac{1}{N} \sum \ln W_{J=0}$  for Monte Carlo events generated with  $J=0,1,2$ . ( $N$  is the number of events of the  $\simeq 131$  MeV line and  $W_J$  is a value of the theoretical formula for the full angular correlation function for spin 0 calculated from the measured angles). The vertical line is the value of the test function for the data. Its distance from the  $J=0$  distribution is a measure for the agreement/disagreement with the spin 0 hypothesis. In this example the confidence level for the hypothesis that the state reached by  $\simeq 131$  MeV photons has  $J=0$  is  $(0.00001 \pm 0.00007)\%$  and therefore can be ruled out.

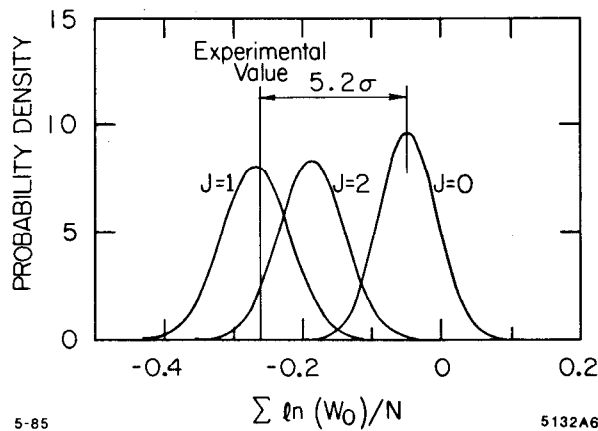


Fig. 11. Likelihood 0 test for the photon line at  $\simeq 131$  MeV (expected spin: 1). The Gaussian distributions are Monte Carlo predictions of the test function under the three spin hypotheses. The vertical line is the value of the test function for the real data.

— A similar result is found for the line at  $\simeq 108$  MeV, where the confidence level for  $J=0$  is  $(0.19 \pm 0.28)\%$ . The data favor the expected spins of  $J=2$  and  $J=1$  for the state reached by the  $\simeq 108$  MeV and  $\simeq 131$  MeV photons respectively, but opposite spin assignments have relatively high probabilities, when each transition is considered independently.

Once spin 0 is ruled out for both lines one can test for the 'global' spin assignment of  $J=2$  and  $J=1$  for the states reached by the  $\simeq 108$  MeV and  $\simeq 131$  MeV photons respectively against the hypothesis  $J=1$  and  $J=2$  for the states reached by the  $\simeq 108$  MeV and  $\simeq 131$  MeV photons respectively. This in effect 'doubles' the statistics available for the test. The combination  $J=2$  and  $J=1$  for the states reached by the  $\simeq 108$  MeV and  $\simeq 131$  MeV photons respectively is favored. The combination  $J=1$  and  $J=2$  for the states reached by the  $\simeq 108$  MeV and  $\simeq 131$  MeV photons respectively has a probability of only  $0.6 \pm^{0.8}_{0.2}\%$  (see Fig. 12). This technique allows only for  $J \leq 2$  values and assumes that the states cannot have the same spins. We also assume that only dipole transitions (E1) occur.

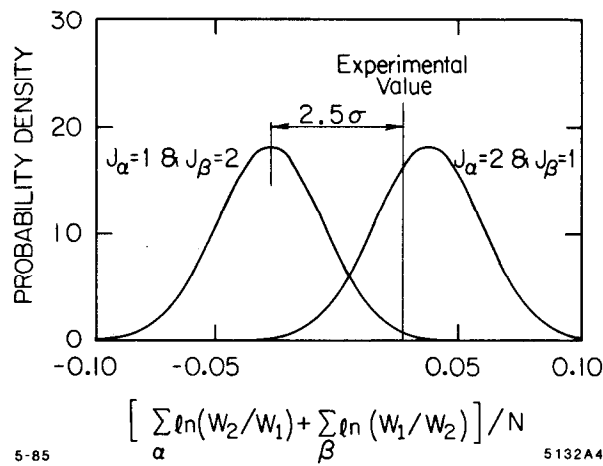


Fig. 12. Likelihood ratio test for the combined data of both lines. The subscript  $\alpha$  denotes the line at  $\simeq 108$  MeV,  $\beta$  stands for the line at  $\simeq 131$  MeV. The expected spins are  $J_\alpha=2$  and  $J_\beta=1$ .

#### 4. Status of the $\zeta(8.3)$ (Ref. 20)

In Summer 1984 the Crystal Ball presented evidence for a new state, called  $\zeta$ , from a study of the inclusive photon spectrum of  $10.4\text{pb}^{-1}$   $\Upsilon(1S)$  data<sup>21</sup>. A photon line was observed at  $(1082 \pm 8 \pm 21)$  MeV corresponding to a mass of  $\simeq 8.3$  GeV/c<sup>2</sup>. The branching ratio was found to be  $B(\Upsilon(1S) \rightarrow \gamma\zeta) \cdot B(\zeta \rightarrow \text{hadrons}) = (0.47 \pm 0.11 \pm 0.26)\%$ . The signal was substantiated by the observation of a second (though less significant) signal at the same mass in a statistical independent sample of low-multiplicity  $\Upsilon(1S)$  decays.

During Autumn 1984 an additional  $22.1\text{pb}^{-1}$  of  $\Upsilon(1S)$  data was accumulated. The inclusive photon spectrum of this second data set is shown in Fig. 13. No signal is observed and a fit gives  $-29 \pm 29$  events at the expected mass of the  $\zeta$  corresponding to an upper limit of  $B(\Upsilon(1S) \rightarrow \gamma\zeta) < 0.8 \cdot 10^{-3}$  (90% C.L.). The low-multiplicity analysis has not yet been completed and will not be discussed here.

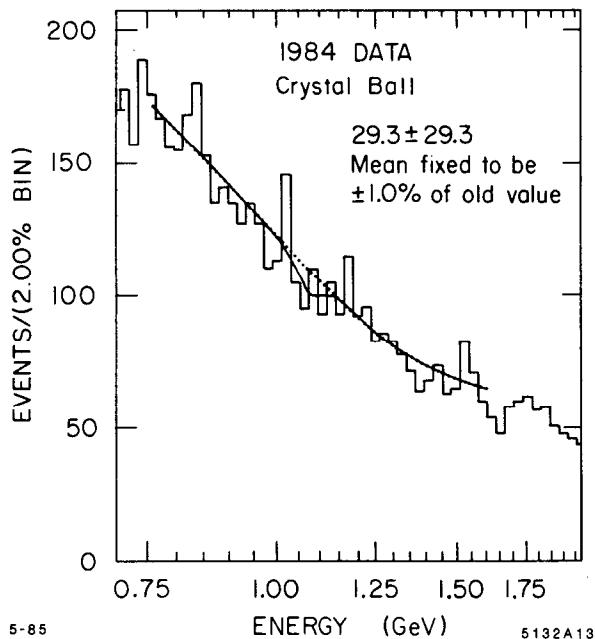


Fig. 13. The inclusive  $\gamma$  spectrum of the  $\Upsilon(1S)$  from the  $22.1\text{pb}^{-1}$  taken in Fall 1984. The best fit is shown with the mean constrained to  $\pm 1\%$  of that expected from the  $\zeta$ .

In order to understand the discrepancy of the two results, extensive quality checks of the 1983 and 1984 data sets have been performed by studying known

signals such as  $\pi^0$ ,  $\eta$ , Bhabha events,  $3\gamma$  QED events etc.. No significant differences are found in the comparison between the two data sets. The tests indicate that we should see the  $\zeta$  in the 1984 data with mean within  $\pm 1\%$  and width within  $\pm 5\%$  of the values found in the 1983 data.

The only difference between 1983 and 1984 data that has been found is the uncorrected hadron yield ( $R_{vis}$ ). The averaged  $R_{vis}$  for 1983 data is 11.1, whereas the average value for 1984 is 12.2. Together with the DORIS beam energy resolution and estimated errors in the  $R_{vis}$  determination this could imply a difference of up to 8 MeV in the center of mass energy between the two data sets. This could be of some importance considering models<sup>22</sup> where the  $\zeta$  peak is due to a radiative decay of some new state close to the  $\Upsilon(1S)$  mass. We estimate that with an 8 MeV shift such models could explain the disappearance of the  $\zeta$  in the 1984 data if this state is 16-26 MeV above the  $\Upsilon(1S)$  (at 90% confidence level).

However ignoring this possibility, and assuming for the following estimate that both data sets are equivalent for studies of  $\Upsilon(1S)$  decays, we combine all our  $\Upsilon(1S)$  data and obtain the spectrum shown in Fig. 14. At the  $\zeta$  mass the fit results in  $67 \pm 30$  events ( $1.9\sigma$ ) giving an upper limit of  $B(\Upsilon(1S) \rightarrow \gamma\zeta) \leq 0.19\%$  (90% C.L.). Work on this problem is continuing.

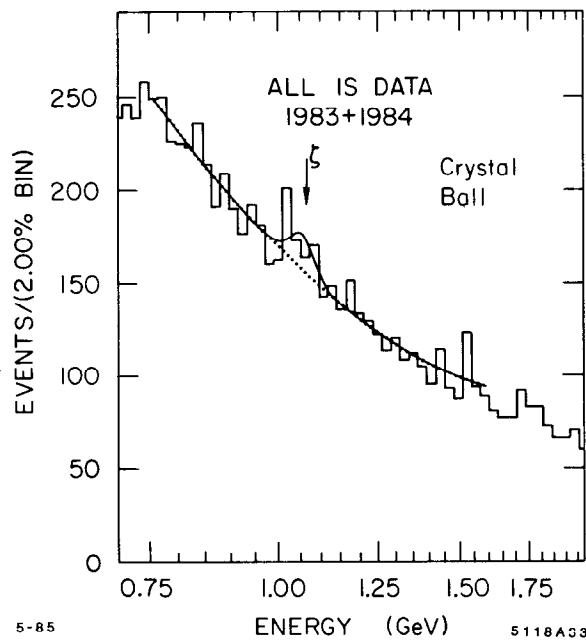


Fig. 14. The inclusive photon spectrum from all available  $\Upsilon(1S)$  data. The fit shown has the mean constrained to  $\pm 1\%$  of that expected for the  $\zeta$ .

## 5. Summary

In summary the Crystal Ball experiment presents a rather complete measurement of the transitions from the  $\Upsilon(2S)$  to the  $\Upsilon(1S)$ .

For the hadronic decay  $\Upsilon(2S) \rightarrow \pi\pi\Upsilon(1S)$  we measure the branching ratios and mass distribution of the  $\pi\pi$  system.

The radiative decays of the  $\Upsilon(2S)$  to the  $\chi_b$  states are measured both in the inclusive photon spectrum and via the  $\gamma\gamma$  exclusive cascade and give consistent results. The transition to the  $^3P_0$  is observed with clear statistical significance. A spin analysis of the exclusive reaction yields results consistent with the expected spins of the  $\chi_b$  states for E1 transitions.

The absence of the  $\zeta$  in the 1984 data is strong evidence against its existence, except for the possibility of beam energy shifts in combination with the existence of a new state close to the  $\Upsilon(1S)$  mass from which the  $\zeta$  is reached by radiative decay.

## References

1. The Crystal Ball Collaboration: D. Antreasyan, D. Aschman, D. Basset, J. K. Bienlein, E. D. Bloom, I. Brock, R. Cabenda, A. Cartacci, M. Cavalli-Sforza, R. Clare, G. Conforto, S. Cooper, R. Cowan, D. Coyne, D. de Judicibus, C. Edwards, A. Engler, G. Folger, A. Fridman, J. Gaiser, D. Gelphman, G. Godfrey, F. H. Heimlich, R. Hofstadter, J. Irion, Z. Jakubowski, S. Keh, H. Kilian, I. Kirkbride, T. Kloiber, W. Koch, A. C. König, K. Königsmann, R. W. Kraemer, R. Lee, S. Leffler, R. Lekebusch, P. Lezoch, A. M. Litke, W. Lockman, S. Lowe, B. Lurz, D. Marlow, W. Maschmann, T. Matsui, P. McBride, F. Messing, W. J. Metzger, B. Monteleoni, R. Nernst, C. Newman-Holmes, B. Niczyporuk, G. Nowak, C. Peck, P. G. Pelfer, B. Pollock, F. C. Porter, D. Prindle, P. Ratoff, B. Renger, C. Rippich, M. Scheer, P. Schmitt, M. Schmitz, J. Schotanus, A. Schwarz, D. Sievers, T. Skwarnicki, K. Strauch, U. Strohbusch, J. Tompkins, H.-J. Trost, R. T. Van de Walle, H. Vogel, U. Volland, K. Wacker, W. Walk, H. Wegener, D. Williams, P. Zschorsch.
2. For a recent review see for example W. Buchmüller, CERN-TH 3938/84, to be published in the proceedings of the International School of Physics of exotic Atoms (Erice, 1984).
3. J. Gaiser, SLAC Report 255 (1982), Ph.D. Thesis, Stanford University, unpublished.
4. R. Nernst, Ph.D. Thesis, Hamburg University, (1985), unpublished.

5. D. Gelphman *et al.*, SLAC-PUB 3563 (1985), to be published in Phys. Rev. D.
6. T. M. Yan, Phys. Rev. D 22 (1980) 1652. Y. P. Kuang and T. M. Yan, Phys. Rev. D 24 (1981) 2874.
7. M. Voloshin and V. Zakharov, Phys. Rev. Lett. 45 (1980) 688.
8. V. A. Novikov and M. A. Shifman, Z. Phys. C 8 (1981) 43.
9. R. Nernst *et al.*, SLAC-PUB 3571 and DESY 85-018 (1985), to be published in Phys. Rev. Lett..
10. W. Walk *et al.*, SLAC-PUB 3575 and DESY 85-019, to be published in Phys. Rev. D..
11. C. Klopfenstein *et al.*, Phys. Rev. Lett. 51, 160 (1983).
12. P. Haas *et al.*, Phys. Rev. Lett. 52, 799 (1984).
13. ARGUS Collaboration, Proc. of the XXII International Conference of High Energy Physics, Leipzig, German Democratic Republic, July 19-25, 1984.
14. At this conference the ARGUS and CLEO groups presented new results concerning the  $\chi_b$  states which now agree with our measurements. Please refer to the contribution of H. Schröder and D. Peterson to these proceedings.
15. E. Eichten and F. Feinberg, Phys. Rev. D 23, 2724 (1981).
16. W. Buchmüller, Phys. Lett. 112B, 479 (1982).
17. P. Moxhay and J. L. Rosner, Phys. Rev. D 28, 1132 (1983).
18. R. McClary and N. Byers, Phys. Rev. D 28, 1692 (1983).
19. T. Skwarnicki *et al.*, Proc. of the XX<sup>th</sup> Rencontre de Moriond: QCD AND BEYOND, March 10-17, 1985, Les Arcs, Savoie, France (to be published by Editions Frontieres).
20. S. Lowe *et al.*, SLAC-PUB 3683 (1985) and Proc. of the XX<sup>th</sup> Rencontre de Moriond: QCD AND BEYOND, March 10-17, 1985, Les Arcs, Savoie, France (to be published by Editions Frontieres). See also E.D. Bloom, Proc. of the 5<sup>th</sup> Workshop in Proton Antiproton Collider Physics, Saint Vincent, Aosta Valley, Italy, February 25 - March 2, 1985.
21. C. Peck *et al.*, SLAC-PUB 3380 (1984) and DESY 84-064 and Proc. of the XXII International Conference of High Energy Physics, Leipzig, German Democratic Republic, July 19-25, 1984.
22. H. Tye and C. Rosenfeld, Phys. Rev. Lett. 53 (1984) 2215.